Effects of Stress-Relieving Heat Treatment on Impact Toughness of Direct Metal Laser Sintering (DMLS)-Produced Ti6Al4V (ELI) Parts

Amos Muiruri, Maina Maringa, Willie du Preez & Leonard Masu

JOM
The Journal of The Minerals, Metals & Materials Society (TMS)

ISSN 1047-4838

JOM
DOI 10.1007/s11837-019-03862-5

Springer

JOM
https://doi.org/10.1007/s11837-019-03862-5

Effects of Stress-Relieving Heat Treatment on Impact Toughness of Direct Metal Laser Sintering (DMLS)-Produced Ti6Al4V (ELI) Parts

AMOS MUIRURI ,[1,3] MAINA MARINGA,[1] WILLIE DU PREEZ,[1] and LEONARD MASU[2]

1.—Department of Mechanical and Mechatronic Engineering, Central University of Technology, Free State, Bloemfontein, South Africa. 2.—Department of Mechanical Engineering, Vaal University of Technology, Vanderbijlpark, South Africa. 3.—e-mail: amos.mwangi.muiruri@gmail.com

The impact toughness of as-built (AB) and stressed-relieved (SR) direct metal laser sintering-produced Ti6Al4V (ELI) was investigated using the standard Charpy impact test over the temperature range of − 130°C to 250°C. Stress-relieving heat treatment was conducted at 650°C for a soaking period of 3 h in argon gas atmosphere. The results showed improvements in the impact toughness after stress-relieving heat treatment. Stress relieving also shifted the established ductile-to-brittle transition temperature to lower temperatures. Comparative analysis of the impact toughness values for AB and SR specimens at ambient temperature showed them to be 48% and 22% lower than recommended values for use in aircraft structures, respectively.

INTRODUCTION

In present-day markets, the need to produce highly efficient products with low lead times, greater customization, and topologically optimized shapes is continuously increasing, prompting the development of new manufacturing techniques. One such technique is production of metal and alloy parts via laser powder bed fusion (LPBF). The use of this additive manufacturing technology in the aerospace and biomedical industries is growing exponentially. However, the transition from production of prototypes to production of real parts is hampered by low confidence in the quality of such parts due to the unproven reliability of LPBF processes. The direct metal laser sintering (DMLS) process is one of the LPBF techniques that is currently being used for production of selected aircraft parts and biomedical implants.[1] The major challenges of this process that have been reported and which could lower confidence in such parts include: (a) the thermal residual stresses developed during the build process due to the high rates of cooling associated with the process, (b) the high surface roughness of the manufactured parts due to partially melted or unmelted powder from the surrounding powder bed, sticking to the surface, as well as the staircase effect, (c) that production of parts free from defects such as porosity requires precise control of a number of process parameters, and finally (d) generation of microstructure different from that found in wrought or cast materials.[1–3] For these reasons, DMLS-produced Ti6Al4V parts have been reported to have mechanical properties different from those of wrought and cast Ti6Al4V; For instance, the yield strength of wrought and cast Ti6Al4V extralow-interstitial (ELI) is 860 MPa and 734 MPa, respectively, while recent literature reported a value for the alloy produced via the DMLS process of 1075 MPa.[3–5] Other than the yield stress, the fatigue and impact toughness properties of parts are also expected to differ because of their different microstructure.

Toughness is a measure of the energy absorbed by a material upon application of a load to fracture. Ductile materials exhibit significant deformation and, therefore, absorb significant amounts of energy before fracture. Brittle materials, on the other hand, are characterized by low ductility and attendant low levels of toughness, thus tending to shatter on impact. In general, materials with high ductility and high strength have good impact toughness.[6] The toughness of engineering materials varies with temperature, and many materials are known to

Published online: 21 October 2019

exhibit a shift from ductile to brittle behavior as the ambient temperature is lowered below a certain point. The temperature at which this shift occurs varies from material to material and is commonly known as the ductile-to-brittle-transition temperature (DBTT).[7] DBTT values are usually determined by Charpy impact tests at various temperatures, using V-notched specimens to control the fracture process by concentrating stress in the area of minimum cross-section. The presence of a notch in a material leads to the generation of a triaxial stress state upon application of load. The prevailing stresses are higher in this case than in a uniaxial or biaxial stress state, thus increasing the chance of failure.[6–7]

Several factors such as defects, grain size, and heat treatment of materials can influence the DBTT. Small grain size and heat treatment that provides grain refinement help to lower the DBTT, thus increasing the range of service temperature of the material. High levels of interstitial elements such as C, O, Mo, and Si shift the DBTT to higher values, thus reducing the range of service temperature of the materials. Anisotropic properties that are observed in rolled or forged products give rise to the absorption of different amounts of energy for specimens with different orientations (depending on the orientation of the v-notch with respect to the rolling and loading direction). The best energy absorption is observed when the v-notch is machined orthogonal to the rolling direction, because the crack induced by stress concentrations at the root of the v-notch tends to propagate across the alignment of the rolling grains/domains upon impact.[7]

There are significant variations in the values of impact energy for the various microstructural states of Ti6Al4V that result from production through traditional methods (casting and casting followed by rolling) at ambient temperatures. Thus, lamellar microstructures have impact energies between 34 J and 49 J, bimodal microstructures between 27 J and 36 J, and equiaxed microstructures between 8 J and 41 J.[8] Lamellar and duplex microstructures show crack-arresting behavior and considerable consumption of energy due to lengthy, stable crack growth. For martensitic and aged microstructures, the overall consumption of energy up to failure is between 4 J and 15 J. After crack initiation, materials exhibit unstable crack growth and only small amounts of energy are absorbed thereafter till failure.[9] Using miniature specimens with dimensions of 5 mm × 5 mm × 27.5 mm, Lee et al.[10] demonstrated that the average impact energy of as-built SLM Ti6Al4V was 6.0 J, while that of heat-treated samples (after stress relieving in argon atmosphere of 650°C for 3 h then furnace cooling) was approximately 7.3 J. Thus, the impact energy in this case was increased by approximately 20% after stress relieving.[11] Lucon and Hrabe[12] focused on the impact properties of additively manufactured Ti6Al4V over the temperature range of − 196°C to 700°C using miniature specimens with dimensions of 24.13 mm × 4.83 mm × 4.84 mm, finding that the v-notch toughness of the AM specimens varied from 2 J to 11.30 J. Those researchers further showed that the DBTT for specimens printed with the open end of the v-notch parallel and orthogonal to the build direction was 187.7°C and 102.6°C, respectively.

There is a dearth of research on the impact properties of DMLS Ti6Al4V (ELI) over a wide range of temperatures as measured using full-size Charpy specimens. The limited literature available fails to address the effects of the characteristics of LPBF techniques (in particular, the DMLS process) on the toughness of produced parts.[10–12] This paper documents an investigation of the effect of stress-relieving heat treatment on the impact properties of DMLS Ti6Al4V (ELI) over temperatures ranging between − 130°C and 250°C. The test specimens used in the work reported herein fell into two categories, viz. AB and SR. The effect of the distribution and sense of residual stresses on the impact toughness of fabricated parts was investigated by printing half of the AB and SR specimens with the open end of the v-notch facing the base plate of the DMLS machine and the other half with the v-notch facing away from the base plate (hereinafter referred to as LO and UP specimens, respectively). The transition curves of DMLS Ti6Al4V (ELI) are presented, the ductile-to-brittle transition temperature (DBTT) is identified, and both are discussed. Fractographs of the fracture surfaces of specimens tested at different temperatures are also presented and analyzed. Moreover, the influence of DMLS process-related defects (porosity) on the fracture properties of the Charpy specimens is investigated using three-dimensional (3D) x-ray micro-computed tomography.

EXPERIMENTAL PROCEDURES

Materials

Atomized powder of Ti6Al4V (ELI) with average powder particle diameter of < 40 μm supplied by TLS Technik GmbH was used to build the Charpy impact test specimens through the DMLS additive manufacturing process. The chemical composition of this material (Supplementary Table S-1) complied with the ASTM F3001-14 standard.[13] The samples were fabricated using an EOSINT M280 DMLS machine with a laser power setting of 175 W, laser diameter of 80 μm, hatch spacing of 100 μm, and layer thickness of 30 μm. A back-and-forth raster scanning pattern with shift angle of 67° after each layer was used to produce the specimens. Argon gas was used as protective inert atmosphere during manufacture. The test specimens were manufactured to the specifications outlined in the ASTM E23-07 standard as illustrated in Fig. 1a. A total of 72 specimens were printed, each with a v-notch, on

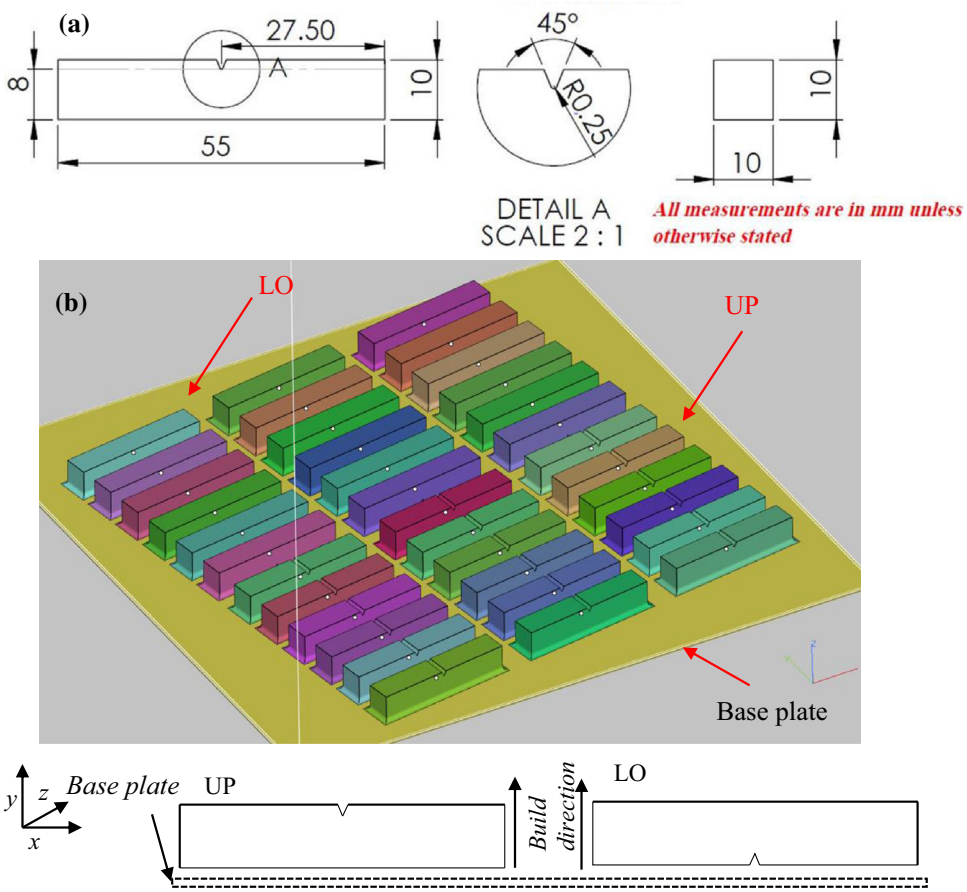

Fig. 1. Schematic diagram showing the (a) specifications and (b) orientation of the notch of the Chary impact samples with respect to the base plate of the UP and LO built specimens.

two separate DMLS machine base plates, with each base plate holding 36 specimens. Half of the specimens on each base plate were printed with the open end of the v-notch facing the base plate (LO) and the rest with the open end of the v-notch facing away from the base plate (UP), as shown in Fig. 1b.

The 36 specimens on one of the base plates were thereafter subjected to stress-relieving heat treatment in argon gas atmosphere at temperature of 650°C with a soaking period of 3 h. The AB and SR specimens were then cut off from the base plate by electrodischarge machining (EDM wire cutting).

Procedures

The Charpy impact test was used to determine the impact toughness of the Ti6Al4V (ELI) specimens at various temperatures by hitting each specimen with a hammer mounted at the end of a pendulum, according to ASTM E23-2007 and ISO 148-1:2009 standards.[14,15] A schematic of the Charpy impact test frame and a mounted specimen is shown in Supplementary Fig. S-1.

In the Charpy test, energy is absorbed as the specimen is broken by a single blow from a pendulum that strikes the middle of the specimen on the surface opposite to the v-notch. The absorbed energy is therefore the fracture energy of each specimen, being read off the dial indicator on the Charpy impact testing machine. A v-shaped notch is generally machined into Charpy impact testing specimens in order to introduce a region of stress concentration in an area with known minimum thickness/cross-section area, thereby ensuring repeatability of the test results.

Testing was conducted at specimen temperatures ranging between − 130°C and 250°C. Except for the temperature of 27°C, which was room temperature at the time of testing, the other test temperatures were obtained by conditioning each specimen by either heating or cooling as appropriate, using an appropriate liquid medium. The medium in the heating bath was constantly agitated, while bringing it to the desired temperature using a H3760-H hot plate for temperatures above room temperature. A water medium was used to generate temperatures in test specimens lying between 50°C and 90°C, while an oil medium was used to generate all other temperatures above 90°C. Temperatures below room temperature were obtained by adding controlled amounts of liquid nitrogen to absolute ethanol in a beaker surrounded by ice, then stirring the mixture until a desired temperature was

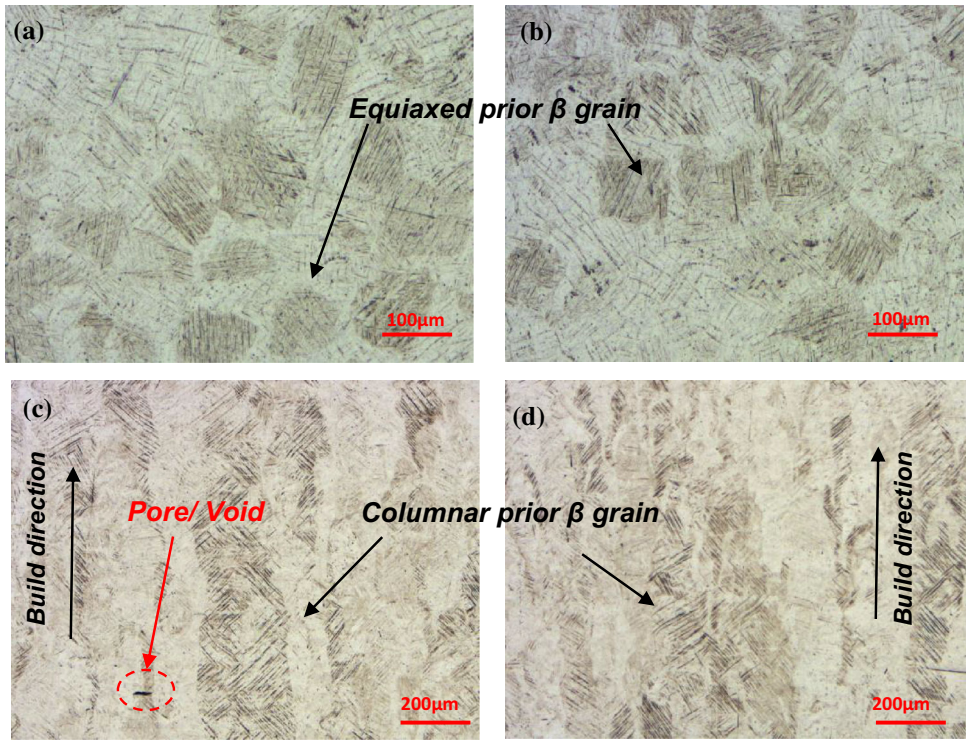

Fig. 2. Optical micrographs of (a) and (c) the as-built (AB) and (b) and (d) stress-relieved (SR) samples for transverse and longitudinal sections with regard to the build direction, respectively.

obtained. The specimens were then soaked at each desired temperature with a tolerance of ± 2°C for a period of at least 15 min before testing. Thermal conditioning of the specimens using water and ethanol as media could influence the impact toughness of the test specimens. However, this was considered a minor concern, since the specimens were kept in the respective baths for short periods of time. Three specimens each were tested at temperatures of − 130°C, − 50°C, 27°C, 90°C, and 200°C, and a single specimen at each of the remaining temperatures. Values of the impact energy absorbed were recorded for all the temperatures and tests done, and their mean and standard deviation calculated, the latter in order to determine the scatter of the results obtained.

The fracture surfaces of the tested specimens were cleaned for a period of 15 min in an ultrasonic cleaner, using ethanol as the cleaning solvent. The surfaces were thereafter dried using a high-pressure stream of compressed air before fractographic analysis.

RESULTS AND DISCUSSION

Microstructure

The optical microstructural images shown in Fig. 2c and d reveal prior β-grains elongated in a direction approximately parallel to the build direction with almost equiaxed grain morphology of β-prior grains in the transverse sections shown in Fig. 2a and b, both before and after heat treatment. Comparison of Fig. 2a and b and Fig. 2c and d reveals no apparent change in microstructure upon stress-relieving heat treatment. The internal microstructure of the columnar/equiaxed grains in the micrographs is seen to be of fine acicular type, which is referred to as α'-martensite. This microstructure results in high tensile strength and low ductility of built parts.

Plastic deformation of the α'-phase is mainly restricted to the basal and prismatic planes of the hexagonal close-packed (hcp) lattice.[16] Since the α' grains do not form colonies of laths sharing the same orientation, as is evident in Fig. 2, the effective slip is confined to a single grain.[16] The microstructure shown in Fig. 2 therefore gives rise to low elongation to failure, which translates to low ductility and low toughness.

Moletsane et al.[4] carried out a similar stress-relieving heat treatment on DMLS Ti6Al4V (ELI) specimens manufactured using the same machine used here. Those authors found that, even though the microstructures were similar prior to and after stress relieving, the ultimate tensile strength (UTS) decreased and the % fracture strain increased, whereas the yield stress remained unchanged after stress relieving.

It can be concluded from these separate studies that AB Ti6Al4V (ELI) will have different mechanical properties when compared with SR Ti6Al4V (ELI). The work presented here attempts to verify

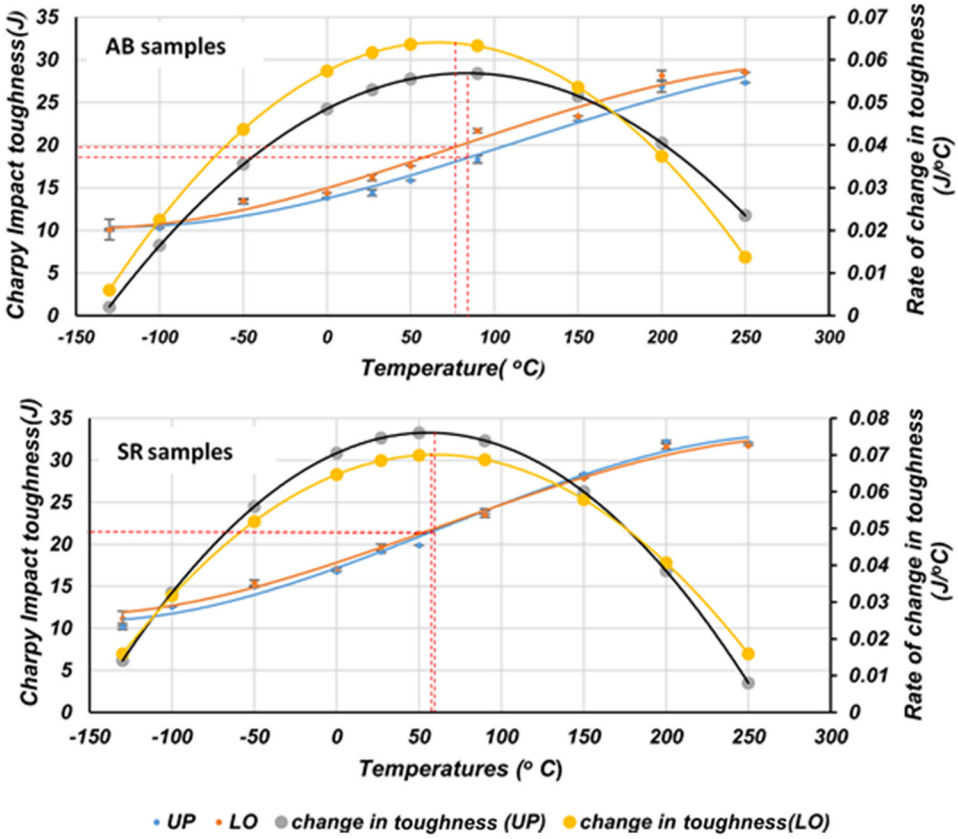

Fig. 3. Charpy impact energy and rate of change in toughness against temperature for AB and SR specimens.

these observations by studying the toughness of both AB and SR specimens, and to determine the degree of change in toughness upon stress relieving.

Comparing the Toughness of LO and UP Specimens

The curves in Fig. 3 show the experimental data points and third-order polynomial best-fit lines for the AB and SR samples tested here. (The recorded values of impact energy and respective standard deviations are presented in Supplementary Tables S-II and S-III.)

The LO, AB specimens are seen in Fig. 3 to have higher values of toughness than the UP specimens over most of the test temperatures. The difference between the curves for the LO and UP specimens demonstrates a clear dependence of the impact toughness on the location of the v-notch with respect to the base plate of the DMLS machine.

In Fig. 3, the difference in the impact energy for the LO and UP, AB specimens is seen to tend to zero at low temperatures, then increase gradually with temperature, before diminishing again at higher temperatures. The rate of change in toughness is seen from the figure to be higher for LO than UP specimens for temperatures in the range of − 150°C to 170°C, but vice versa beyond 170°C.

The general trend of the curves in Fig. 3, for the SR samples, is similar to that exhibited by the curves for the AB samples; the curves of the notch impact toughness increase with increasing temperature, with a point of inflection in each case. The results for the SR samples show very small differences between the impact toughness values at the same temperature for the two cases of the UP and LO specimens, with overlapping standard deviations. This unexpected but much smaller difference in the mean values (≤ 5%) may be associated with the presence and distribution of residual stresses in the SR specimens, likely arising from their separation from the base plate.

The distribution of residual stress in DMLS-produced parts varies with the height and shape of the component. Mercelis and Kruth[17] demonstrated that the distribution of residual stresses in the *Z*-built direction for a part removed from the base plate consists of a zone of tensile stresses at and just below the upper surface, a zone of compressive stress in the central region, and a zone of tensile stress at and just above the bottom surface. The results of Mugwagwa et al.[18] and Van Zyl et al.[19] were consistent with those of Mercelis and Kruth,[17] demonstrating that the tensile residual stresses were maximum on the upper surface. These maximum residual stresses for the two cases of DMLS

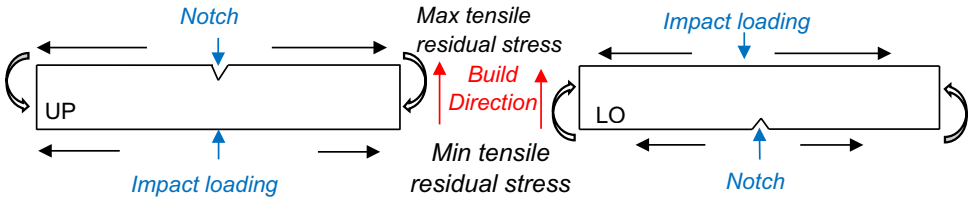

Fig. 4. State of residual stresses prevalent in UP and LO specimens in relation to applied impact load.

UP and LO specimens are illustrated schematically in Fig. 4.

From this figure and the general theory of bending of beams, upon impact, the surface bearing the v-notch and the impacted surface of the specimens in both cases shown in Fig. 4 experience tensile and compressive longitudinal direct stresses, respectively. According to the foregoing theory, the effect of residual stresses in the AB samples that are related to the *Z*-build direction is to increase the effective tensile longitudinal direct stresses on the surfaces bearing the notch for the UP specimens, by a higher value than for the LO specimens.

Therefore, for the same impacting pendulum and weight (same imparted energy of 297 J and constant impact velocity of 5.2 m/s, in this case), the resistance to the impacting load will be slightly less for the UP than LO specimens. The UP specimens will therefore fail at lower impact values than the LO specimens. This inference is supported by the curves of impact energy presented in Fig. 3 for both the AB and SR specimens, with the former showing significant differences that are ≤ 18% of the lower value for the UP specimens over the curve range in comparison with the very small differences that are ≤ 7% in the latter case. At the ambient temperature of 27°C the average impact energies of the AB, UP and LO specimens were recorded as 14.11 ± 0.36 J and 16.18 ± 0.38 J, respectively, with a difference of 2.07 J between the mean values. Upon stress-relieving heat treatment, the difference in impact energy between the UP and LO specimens at the same test temperature diminished to ≤ 5% of the lower value for UP specimens. At the ambient temperature of 27°C, the values of impact energy recorded for SR, LO and UP specimens were 19.64 ± 0.17 J and 19.13 ± 0.37 J, respectively, with a difference of 0.51 J between the mean values. From the foregoing analysis, it is evident that the effect of the built direction and resulting distribution of residual stresses in the DMLS process cannot be ignored. Although x-ray diffraction (XRD) scanning could have shed more light on the state of surface and subsurface residual stresses, this lay outside the scope of the work whose results are presented here.

The two forms of Ti6Al4V (ELI) alloy did not show drastic changes in the magnitude of the notch toughness with increase in the test temperature (Fig. 3), with the maximum change in both cases being less than 0.08 J/°C. It was not possible to establish the upper shelf of the transition curves using the obtained and plotted data for the impact toughness in the present work. Therefore, it is not possible to determine the fracture transition plastic (FTP) temperature, i.e., the temperature at which the material exhibits 100% macroscopic ductile failure, within the temperature range used for testing here. Nevertheless, it is possible to determine the DBTT, viz. the lower service temperature of the material. Typically, the DBTT identifies the point at which the percentage macroscopic brittle and ductile areas are almost equal. In other words, it is the point of inflection of the transition curves. To accurately locate the point of inflection (DBTT), the gradient of the fit toughness curves shown in Fig. 3 were plotted together with the related curves of toughness. The temperatures at which the gradient of the curves for the rate of change in notch toughness becomes zero in the graphs denotes the DBTT of the material. The rate of change of toughness with temperature for both LO and UP, AB specimens, for example, is seen to increase to a maximum of 0.065 J/°C and 0.057 J/°C for LO and UP specimens, respectively, at corresponding temperatures of 80°C and 85°C, and to decrease at a faster rate for the LO specimens. The analysis of the curves of the gradient shown in Fig. 3 is summarized in Supplementary Table S-IV.

The effects of the stress-relieving heat treatment and the location of the v-notch of the test specimen with respect to the DMLS base plate on the DBTT are clearly manifested in Fig. 3 and in Supplementary Table S-IV. The values in the table show a shift in DBTT to the left (low temperature) for the SR specimens in relation to the AB specimens, and for the LO specimens in relation to the UP specimens. It can thus be concluded that the effect of residual stresses and the location of the v-notch with respect to the residual stresses results in a reduction in the DBTT temperature in both cases. It is also noted that, at the transition temperatures, the DBTT toughness of both AB and SR, LO specimens are higher than those of the UP specimens (Supplementary Table S-IV).

Comparing the Toughness of AB and SR Specimens

Figure 5 shows the data with standard deviations for cases where three specimens were tested in the

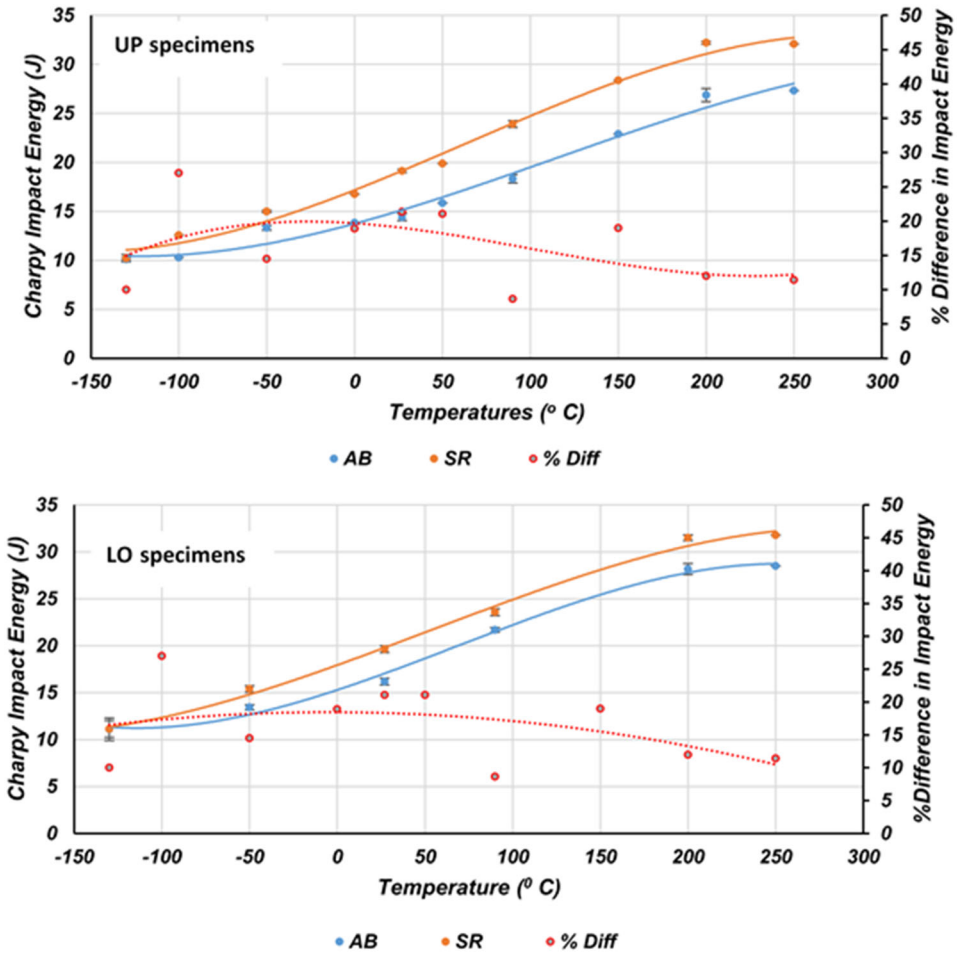

Fig. 5. Comparison between AB and SR specimens.

same load and temperature regime and the fit curves of toughness for the two forms of DMLS Ti6Al4V (ELI) alloy (AB and SR) specimens on the same graphs, one for the UP and the other for the LO specimens. From the curves in these two figures, the effect of the stress-relieving heat treatment is seen to have greatly improved the impact toughness of the specimens. This is evident from the fact that the data and fit curves for the SR specimen in both figures are seen to have shifted upwards along the y-axis (the axis for impact toughness). It is apparent from the curves in the two figures that, for all the temperatures except − 130°C, the values of the notch toughness for SR specimens are significantly higher than those of the AB samples. The % difference in impact energy between the two forms of the alloy range from 1.2% to 32.8% for the UP specimens but from 10% to 27% for the LO specimens. The percentage difference is seen to vary with temperature for both the UP and LO specimens, from a minimum at low temperatures through to a maximum with increasing temperature, and reducing in magnitude beyond that.

The energy absorbed in fracturing the specimens at the lowest temperature of − 130°C of the test for the two forms of the alloy was recorded as 10.09 J and 10.11 J for the AB, UP and LO specimens, respectively, and 10.21 J and 11.14 J for the SR, UP and LO specimens, respectively. These values are 70% and 62% of the values of the impact toughness at room temperature for the AB, UP and LO specimens, respectively, and 56% and 59% of the values of impact toughness at room temperature for the SR, UP and LO specimens, respectively. This is a positive finding, as it indicates that the as-built and stress-relieved DMLS Ti6Al4V (ELI) still retain appreciable notch impact fracture toughness even at subzero temperatures. It is worth noting that the AB specimens consist of α'-phase (acicular martensitic structure) which exists as hcp crystals. This is also the case for the SR specimens, since stress-relieving heat treatment at 650°C for 3 h did not alter or decompose the martensitic structure, as is evident in Fig. 2, which partly shows sections of the microstructure of an SR specimen.

The α'-phase (acicular martensitic structure) of Ti6Al4V has an hcp structure similar to that of the α-phase and a slip direction along the axes of an even order ($\langle 11\bar{2}0 \rangle$).[9] Such slip directions are along closely packed planes. This results in small Peierls

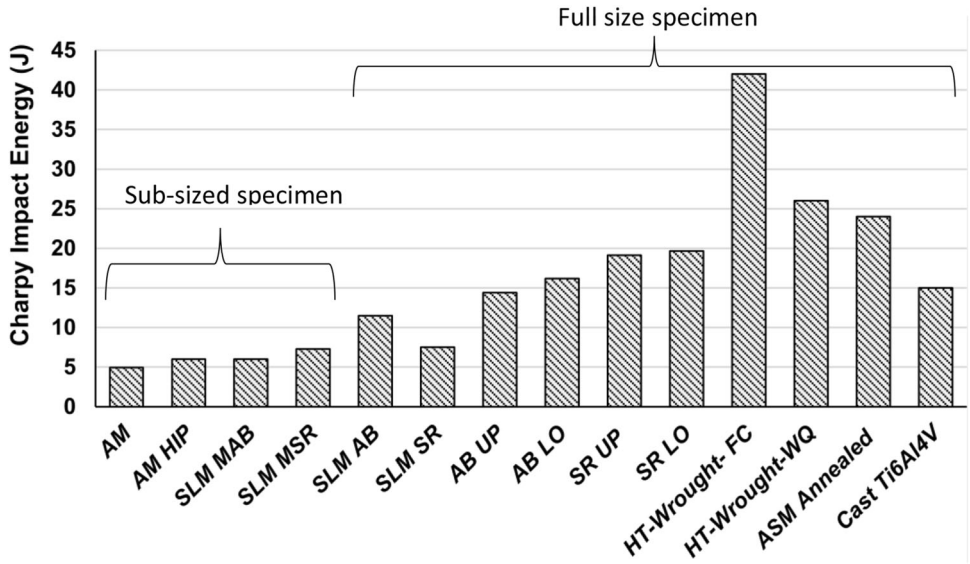

Fig. 6. Comparison of Charpy impact toughness of various forms of Ti6Al4V produced using different various processes.[8,10–12,22,23]

barriers and weak elastic interaction of dislocations with point defects in a manner similar to all face-centered cubic (fcc) structures with axes of an even order ⟨110⟩,[20] hence the lack of low-temperature embrittlement. Comparative analysis of the toughness data obtained in this research for a full-size DMLS Ti6Al4V Charpy specimen with data published in various articles for both full-size and miniature Charpy specimens shows disparities (Supplementary Table S-V); the data are presented in Fig. 6.

Ti6Al4V alloy has different values of toughness for different thermal processing conditions and sizes of test specimen, as shown in Fig. 6. The work of Yana et al.[11] using full Charpy specimens gave lower values compared with the current research. Using miniature Charpy specimens (MAB and MSR), Lee et al.[10] obtained lower values than those obtained in the current research. Rzepa et al.[21] observed that the toughness values obtained for Charpy impact specimens with subsized geometries are normally lower than those obtained with full-size Charpy specimens. Nevertheless, Lee et al.[10] demonstrated a 20% increase in toughness upon stress-relieving heat treatment, which is less than the 32% increase obtained in the present work. It is expected that the mechanical properties of parts prepared using different AM systems may differ slightly as a result of the use of different process parameters, which may influence the porosity, microstructure, and surface roughness and therefore the mechanical properties of the produced parts. Other processes such as hot isostatic pressing (HIP) can be used to improve the toughness of additively manufactured parts, as is evident from Fig. 6. The American Society of Metals (ASM)[22] specifies that Ti6Al4V (ELI) for use in aircraft structures should have a Charpy v-notch toughness value of at least 24 J. This is approximately 66% and 48% higher than the values for the AB (UP and LO) specimens, respectively, and 25% and 22% higher than the values for the SR (UP and LO) specimens, respectively, obtained in the present work. With the exception of the work by Lee et al.,[10] it is evident from the data presented in Fig. 6 that the toughness of DMLS Ti6Al4V (ELI) is improved upon heat treatment, including stress-relieving heat treatment that does not lead to a transformation of the martensitic microstructure.

Three-dimensional (3D) x-ray micro-computed tomography (micro CT) analysis of the porosity of one of a number of broken halves arising from testing carried out in the present work at various selected temperatures is shown in Fig. 7. The color code bar of the porosity in the 3D view in the figure shows different pore sizes (0.060 μm to 1.36 μm) in the sample. From the color codes, the pores near the fracture surface are seen to lie in the same size range as those far from it. This would imply that, although playing a role in the eventual failure of the specimens, the pores were not critical in the initiation of failure, which was rather a result of the stress-concentrating effect of the v-notch. The summary of the percentage defect ratio in the broken halves to the material volume at various test temperatures in Supplementary Table S-VI demonstrates that the percentage densification of the DMLS Ti6Al4V (ELI) in both the as-built and stress-relieved form was approximately 100%.

The fracture surface consisted mainly of the flat region, normal to the applied longitudinal tensile stress, and the plane of high stress shear (shear lips), which is slanted to the same applied tensile longitudinal stress (Supplementary Figs. S-2, S-3). The shear lip areas were observed to increase with the test temperature in the AB and SR specimens,

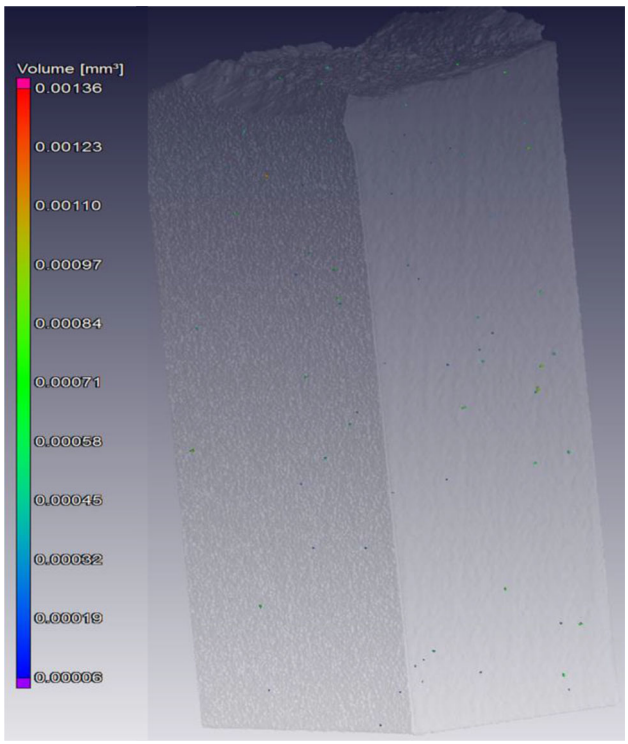

Fig. 7. Sample of distribution of pores on half-specimen of DMLS Ti6Al4V (ELI) after Charpy loading.

while the flat areas decreased. This is an indication of the increase in material ductility with temperature. It is worth noting, however, that the overall fracture energy is dependent not only on the shear area but more so on the microscopic fracture mechanism in the macroscopic brittle area. Therefore, the increase in the shear fracture area with temperature can only partly explain the increase in notch toughness.

Defects such as those seen in Fig. 8a as well as in the 3D view in Fig. 7 may arise due to lack of fusion caused by the laser beam being unable to fully melt and consolidate pockets of powder in between consecutive layers.

Figure 8a and c shows a typical fracture surface of one of the specimens tested here, at the flat surface area.

The fracture surface appears macroscopically brittle (a term used here to designate crack propagation in a direction normal to that of the existing direct stresses). Microscale examination of the flat portion and the walls of the cups shown in the images revealed dimples. This is also common in uniaxially loaded ductile tensile specimens. Figure 8b and d shows typical micrographs of the shear fracture area (shear lips) of one fracture sample each of the AB and SR specimens tested here. The micrographs highlight the presence of elliptical

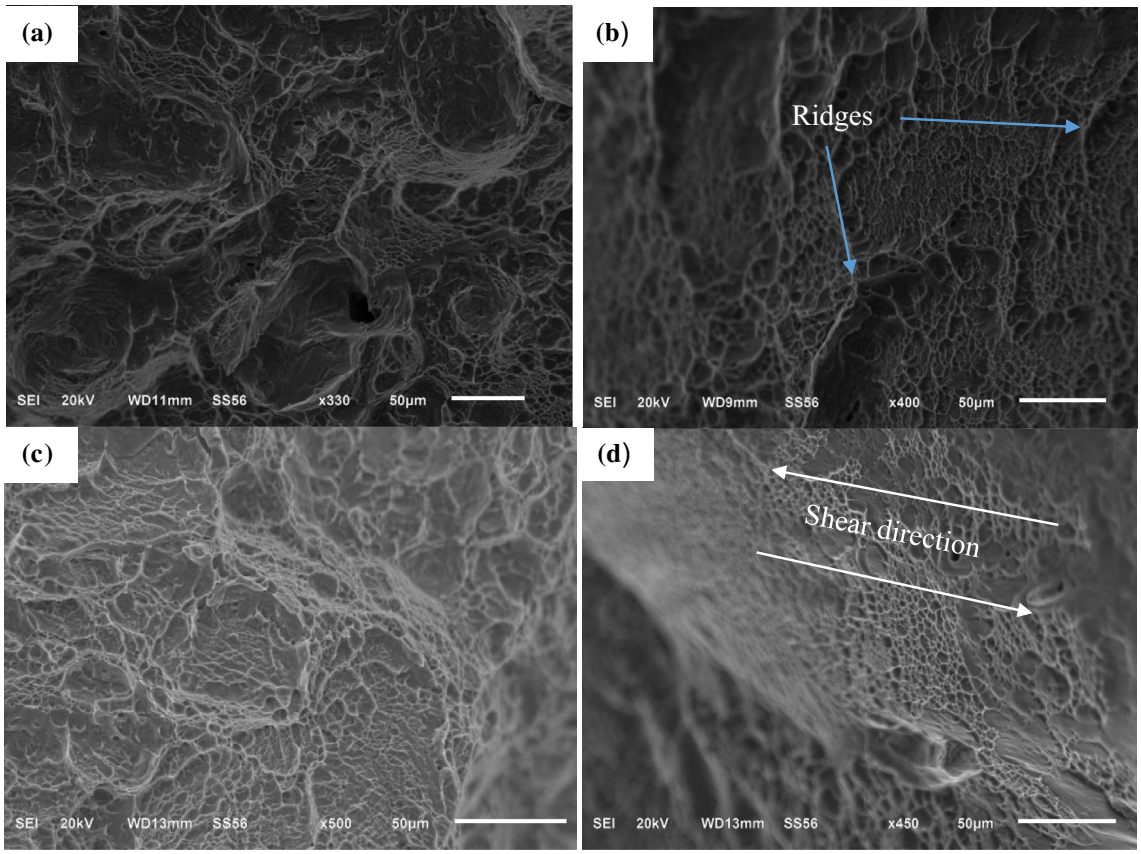

Fig. 8. SEM SE images of (a, c) the flat region (plane-strain mode of failure) and (b, d) shear lip (high-shear-stress mode of failure) for AB and SR samples.

dimples and ridges that are aligned in the direction of shear. The fact that there is no concentration of pores around the fracture surfaces, as is evident in Fig. 7, in addition to the known effect of stress concentration around discontinuities supports the supposition that the failure of the Charpy specimens was primarily due to cracks initiating from the root of the v-notch. The effect of this material's porosity on the energy of fracture (toughness) can therefore be ignored, despite the occurrence of some pores/voids on the fracture surfaces as shown in Fig. 8.

CONCLUSION

The results of Charpy impact tests on DMLS Ti6Al4V (ELI) specimens were analyzed and discussed, with the following conclusions:

(a) The LO, AB DMLS Ti6Al4V (ELI) specimens showed higher values (≤ 18%) of notch toughness in comparison with the UP, AB DMLS Ti6Al4V (ELI) specimens. The effect of the location of the v-notch with respect to the base plate was in contrast minimal (≤ 5%) for the stress-relieved samples.

(b) The presence and distribution of residual stress in the AB samples gave rise to lower values of DBTT for the LO than UP specimens. Stress-relieving heat treatment shifted the DBTT to even lower values: from 74°C (LO) and 80°C (UP) to 58°C (LO) and 60°C (UP).

(c) The DBTT toughness of the AB, LO specimens was higher than that of UP specimens. Upon stress-relieving heat treatment, the values of DBTT toughness were more or less the same for the UP and LO specimens.

(d) The AB and SR DMLS Ti6Al4V (ELI) specimens were observed to still retain considerable values of toughness even at a temperature of − 130°C, viz. about 70% and 56% of the energy absorbed at room temperatures for the AB and SR, respectively.

(e) The densification of the built DMLS parts was ∼ 100%, and the distribution of pores did not show higher incidences near or around the sites of eventual fracture.

(f) The fracture surfaces of the tested specimens consisted of regions of plane strain (flat regions) and high shear stress (shear lips). The magnitude of the flat fracture surface area decreased at high temperature, while the shear lips surface area increased, indicating an increase in ductility.

(g) The v-notch toughness values obtained in this research at ambient temperature were 48% and 22% lower for AB and SR specimens, respectively, than the value of 24 J recommended for use in the aerospace industry.

(h) The results presented herein show that stress-relieving heat treatment improves the toughness of as-built DMLS Ti6Al4V (ELI). However, this heat treatment regime is not sufficient to attain the toughness value recommended for use in the aircraft industry. Future research should aim at developing an ideal microstructure with optimum strength and ductility and therefore enhanced toughness through further heat treatment after stress relieving.

ACKNOWLEDGEMENTS

The active support and funding of the South African Department of Science and Technology through the CSIR for the Titanium Centre of Competence and the Collaborative Program in Additive Manufacturing, Contract No. CSIR-NLC-CPAM-15-MOA-CUT-01, are gratefully acknowledged. The authors also acknowledge the CRPM for building the test specimens through DMLS. The Department of Mechanical Engineering of the University of Pretoria is also acknowledged for providing the facilities that were used for testing.

CONFLICT OF INTEREST

The authors declare that they have no conflicts of interest.

ELECTRONIC SUPPLEMENTARY MATERIAL

The online version of this article (https://doi.org/10.1007/s11837-019-03862-5) contains supplementary material, which is available to authorized users.

REFERENCES

1. F.I. Azam, M.A. Rani, T.V. Rao, A. Khurram, and H.A. Zaharin, *Mater. Sci. Eng.* (2018). https://doi.org/10.1088/1757-899X/328/1/012005.
2. A.E. Patterson, S.L. Messimer, and P.A. Farrington, *Technologies.* 5, 15 (2017).
3. H.K. Rafi, N.V. Karthik, H. Gong, T.L. Starr, and B.E. Stucker, *J. Mater. Eng. Perform.* 22, 3872 (2013).
4. G. Moletsane, P. Krakhmalev, A. Du Plessis, I. Yadroitsava, I. Yadroitsev, N. Kazantseva, and S. Arf, *J. Ind. Eng.* 27, 110 (2016).
5. T.M. Mower and M.J. Long, *Mater. Sci. Eng. A* 651, 198 (2015).
6. C. Fischer and C. Antony, *Introduction to Contact Mechanics*, 2nd ed. (New York: Springer, 2007), pp. 49–70.
7. G. Dieter, *Mechanical Metallurgy*, 3rd ed. (New York: McGraw-Hill Book. Co., 1986), pp. 471–499.
8. C. Buirette, J. Huez, N. Gey, A. Vassel, and E. Andrieu, *Mater. Sci. Eng. A* 618, 546 (2014).
9. G. Lütjering, *Mater. Sci. Eng. A* 243, 32 (1998).
10. K. Lee, Y. Kim, H. Yu, S. Park, and C. Kim, *Arch. Metall. Mater.* 62, 1341 (2017).
11. E. Yasa, D. Jana, K. Jean, and R. Marleen, *Virtual Phys. Prototyp.* 5, 89 (2010).

12. E. Lucon and N. Hrabe, *Applied Chemicals and Materials Division Materials Measurements Laboratory,* NIST Technical Note 1936 (2016).
13. ASTM F3001-14, *Standard Specification for Additive Manufacturing Titanium-6 Aluminium-4 Banadium Extra Low Interstitial (ELI) with Powder Bed Fusion*.
14. ASTM E23-07, *Standard Test Methods for Notched Bar Impact Testing for Metallic Material* (ASTM International, West Conshohocken, 2007).
15. South African National Standard (SANS), *Metallic Materials—Charpy Pendulum Impact Test*, 2nd ed. (Pretoria: SABS Standard Division, 2013).
16. D. Banerjee and J. Williams, *Acta Mater.* 61, 844 (2013).
17. P. Mercelis and J.-P. Kruth, *Rapid Prototyp. J.* 12, 254 (2006).
18. L. Mugwagwa, D. Dimitrov, S. Matope, and A.M. Venter, *18th RAPDASA 2017 Conference Proceedings 153* (2017).
19. I. Van Zyl, I. Yadroitsava, I. Yadroitsev, and S. Afr, *J. Ind. Eng.* 27, 134 (2016).
20. V.M. Chernov, B.K. Kardashev, and K.A. Moroz, *Nucl. Mater. Eng.* 9, 496 (2016).
21. S. Rzepa, T. Bucki, P. Konopík, J. Džugan, M. Rund, and R. Procházka, *IOP Conf. Ser. Mater. Sci. Eng.* (2017). https://doi.org/10.1088/1757-899x/179/1/012063.
22. ASM. Aerospace Specification Metals Inc. http://asm.matweb.com/search/SpecificMaterial.asp?bassnum=MTP643. 02 Dec 2018.
23. ASM International, *Material Properties Handbook: Titanium Alloys* (Material Park: ASM International, 1994)ISBN 978-0-87170-481-8.